HHS Public Access

Author manuscript

J Invest Dermatol. Author manuscript; available in PMC 2019 January 01.

Published in final edited form as:

J Invest Dermatol. 2018 January ; 138(1): 179–188. doi:10.1016/j.jid.2017.07.847.

The Role of Fibroblast Growth Factor Binding Protein 1 in Skin Carcinogenesis and Inflammation

Marcel Oliver Schmidt[1,*], **Khalid Ammar Garman**[1], **Yong Gu Lee**[1,2], **Chong Zuo**[1,3], **Patrick James Beck**[1,4], **Mingjun Tan**[1], **Juan Antonio Aguilar-Pimentel**[5], **Markus Ollert**[6], **Carsten Schmidt-Weber**[7], **Helmut Fuchs**[5], **Valerie Gailus-Durner**[5], **Martin Hrabe de Angelis**[5,8,9], **German Mouse Clinic Consortium**[§], **Elena Tassi**[1], **Anna Tate Riegel**[1], and **Anton Wellstein**[1,*]

[1]Lombardi Comprehensive Cancer Center, Georgetown University, Washington, DC 20057, USA

[2]Purdue University System, Department of Chemistry West Lafayette, IN, USA

[3]Washington University in Saint Louis School of Medicine, Department of Medicine Saint Louis, MO, USA

[4]Thomas Jefferson High School for Science and Technology, Chemistry Alexandria, VA, USA, 703-750-8300

[5]German Mouse Clinic, Institute of Experimental Genetics, Helmholtz Zentrum München, German Research Center for Environmental Health, Ingolstädter Landstraβe 1, 85764 Neuherberg, Germany

[6]Department of Infection and Immunity, Luxembourg Institute of Health, Esch-sur-Alzette, Luxembourg, and Department of Dermatology and Allergy Center, Odense Research Center for Anaphylaxis, University of Southern Denmark, Odense, Denmark

[7]Center of Allergy & Environment (ZAUM), Technische Universität München (TUM) and Helmholtz Zentrum, Biedersteiner Str. 29, 80802 Munich, Germany, and Member of the German Center for Lung Research (DZL), Aulweg 130, 35392 Gieβen, Germany

[*]correspondence to: Marcel O. Schmidt; mos6@georgetown.edu, Phone: +1 (202) 687-4771, fax; +1 (202) 687-4821, Lombardi Comprehensive Cancer Center, Georgetown University, Washington, DC 20057, USA; or Anton Wellstein; anton.wellstein@georgetown.edu, Phone: +1 (202) 687-3672, fax; +1 (202) 687-4821, Lombardi Comprehensive Cancer Center, Georgetown University, Washington, DC 20057, USA.

[§]A full list of consortium members appears at the end of the paper.

The work for this manuscript was done in Washington, DC, USA and Munich, Bavaria, Germany

Conflict of Interest: The authors state no conflict of interest.

[§]German Mouse Clinic, Helmholtz Zentrum München, German Research Center for Environmental Health GmbH, Neuherberg, Germany

Lore Becker1,3, Alexandra Vernaleken1,3, Thomas Klopstock3,12,13,16,17, Thure Adler1, Irina Treise1, Dirk H. Busch 2, Marion Horsch1, Johannes Beckers1,14,15, Kristin Moreth1, Raffi Bekeredjian4, Lillian Garrett1,6, Sabine M. Hölter1,6, Annemarie Zimprich1,6, Wolfgang Wurst 6,11,12,13, Robert Brommage1, Wolfgang Hans1, Oana Amarie1,6, Jochen Graw 6, Jan Rozman 1,15, Martin Klingenspor7,8, Julia Calzada-Wack1,5, Patricia da Silva-Buttkus1,5, Frauke Neff1,5, Ildiko Racz1,9, Andreas Zimmer9, Birgit Rathkolb 1,10,15, Eckhard Wolf 10, Manuela Östereicher1, Ralph Steinkamp1, Christoph Lengger1, Holger Maier1, Claudia Stoeger1, Stefanie Leuchtenberger1

[8]Chair of Experimental Genetics, Center of Life and Food Sciences Weihenstephan, Technische Universität München, Germany

[9]German Center for Diabetes Research (DZD), Ingolstädter Landstraße 1, 85764 Neuherberg, Germany

Abstract

Fibroblast growth factor-binding protein 1 (FGFBP1, FGF-BP) is a secreted chaperone that mobilizes paracrine-acting FGFs, stored in the extracellular matrix, and presents them to their cognate receptors. FGFBP1 enhances FGF signaling including angiogenesis during cancer progression, and is upregulated in various cancers. Here we evaluated the contribution of endogenous FGFBP1 to development and homeostasis as well as to skin pathologies utilizing Fgfbp1-knockout (KO) mice. Relative to wild-type (WT) littermates KO mice showed no gross pathologies. Still, in KO mice a significant thickening of the epidermis associated with a decreased transepidermal water loss and increased pro-inflammatory gene expression in the skin was detected. Also, skin carcinogen challenge by DMBA/TPA resulted in delayed and reduced papillomatosis in KO mice. This was paralleled by delayed healing of skin wounds and reduced angiogenic sprouting in subcutaneous matrigel plugs. Heterozygous GFP-knock-in mice revealed rapid induction of gene expression during papilloma induction and during wound healing. Examination of WT skin grafted onto Fgfbp1 GFP knockin reporter hosts and bone marrow transplants from the GFP reporter model into WT hosts revealed that circulating Fgfbp1-expressing cells migrate into healing wounds. We conclude that tissue-resident and circulating Fgfbp1-expressing cells modulate skin carcinogenesis and inflammation.

Keywords

Carcinogenesis; Wound healing; FGF; Angiogenesis; Inflammation

Introduction

The fibroblast growth factor binding protein (FGFBP) family consists of three human and two murine (FGFBP1, 3) members, which are secreted chaperone proteins that bind to FGFs and enhance their biological activity (Tassi and Wellstein 2006). As the best characterized member, FGFBP1 has been shown to bind to FGF1, 2, 7, 10 and 22 in a reversible manner through its C-terminal domain (Tassi et al. 2011). Paracrine FGFs (e. g. FGF1 and FGF2) are immobilized in the extracellular matrix and are released to bind to their cognate FGF receptors. In this context FGFBP1 works as a modulator that chaperones the FGFs from their location in the extracellular matrix to target cells expressing FGF receptors.

FGFBP1 is expressed in epithelial cells in skin, stomach, eye, ileum and colon (Aigner et al. 2002; Kurtz et al. 1997), was found to act as an angiogenic switch molecule in cancer (Czubayko et al. 1997) and expressed in squamous cell carcinoma (Czubayko et al. 1994), pancreatic and colon cancer (Henke et al. 2006). Also, FGFBP1 is upregulated during a two-step chemical skin carcinogenesis challenge with DMBA and TPA (Kurtz et al. 2004). We have previously investigated the role of FGFBP1 in a transgenic mouse model and found

that conditionally expressed FGFBP1 accelerated angiogenesis in subcutaneously implanted matrigel plugs, enhanced wound healing and reduced ischemic hindlimb injury. Furthermore, FGFBP1 and FGFBP2 play a critical role during chicken development: knockdown of either of them caused embryonic lethality in part through vascular leakage. (Gibby et al. 2009).

To investigate the function of endogenous FGFBP1 we generated a knockout and a knock-in GFP-reporter mouse model, to investigate the role of FGFBP1 in development, skin homeostasis and repair and during challenge by chemical carcinogenesis.

Results

Generation of Fgfbp1-knockout mice

The complete Fgfbp1 open-reading-frame contained in exon 2 on chromosome 5 was replaced by a floxed Fgfbp1 gene and a neo-GFP cassette, resulting in $Fgfbp1^{+/loxP\text{-}neo\text{-}gfp}$ mice, which were then crossed with mice expressing cre (Fig. 1a). The resulting mouse line expressed GFP in lieu of Fgfbp1 ($Fgfbp1^{+/gfp}$) and served to monitor activity of the Fgfbp1 promoter. To generate Fgfbp1-knockout mice (KO) the $Fgfbp1^{loxP\text{-}neo\text{-}gfp}$ mice were crossed with mice expressing the recombinase Flpase and then with cre-expressing mice (Fig. 1b-f). The mouse strain in this study is primarily C57Bl/6N and to a lower degree SV129N.

The epidermis of KO mice is thicker and has a reduced permeability

Since endogenous FGFBP1 is predominantly expressed in skin (Aigner et al. 2002), we initially focused on the analysis of the skin phenotype in the KO animals. The epidermis of adult (2-3 months old) but not juvenile KO mice (3 weeks old) showed a twofold increased thickness ($p<0.05$; Fig. 2a, S1a). In contrast, the thickness of dermis, fat and panniculus muscle were not significantly different between WT and KO (Fig. 2b). The increased thickness in KO mice coincided with an increased proliferation index in basal keratinocytes (Fig 2c, e). Also, ~50% of the epidermis in KO mice showed multiple nucleated keratinocyte strata in contrast with a mostly single basal layer in WT (Fig. 2d). Commensurate with epidermal thickening in KO mice transepidermal water loss (TEWL) was decreased (Fig. 2f). Also, global expression analysis of skin RNA, indicates significantly altered pathways related to barrier function in KO versus WT mice (Fig. S2a) although staining for Claudin1 and Filaggrin showed no differences in the epidermis between WT and KO (Fig. 2e). Analysis of RNA from the epidermis and from the dermis showed a higher expression of the macrophage marker F4/80 and Ffgr1c in the epidermis of KO mice (Fig. 2g). In KO mice both Fgfr1b and c are expressed at similar levels in the dermis and epidermis, whilst a 10-fold higher expression of the c-isoform was seen in the dermis vs the epidermis of WT animals (Fig. 2g). Fgf7 and Fgfr2 were not differentially expressed in the epidermis or dermis (Fig. S1b).

FGFBP1 upregulation in patients' psoriatic lesions and squamous cell skin cancer (SCC)

Epidermal thickening observed in the Fgfbp1-KO model has been described in inflammatory pathologies of the skin such as psoriasis (Stern 1997) and FGFR2 and FGF7 were found elevated in psoriatic skin (Guban et al. 2016). To assess FGFBP1 gene expression we

analyzed two previously published gene expression studies (Nair et al. 2009; Reischl et al. 2007) of paired samples of normal skin, psoriatic skin without and with lesions. FGFBP1 is significantly upregulated in lesions but not in unaffected skin (Fig. S3a, b). Analysis of another study (Nindl et al. 2006) revealed that FGFBP1 is upregulated in actinic keratosis (AK) and invasive SCC relative to normal skin (Fig. S3c).

Skin epidermis of KO mice shows elevated pro-inflammatory gene expression

A psoriatic phenotype can be mimicked in mice by topical application of Aldara, a pro-inflammatory agent (Walter et al. 2013) Fig. 3a). Aldara contains Imiquimod and activates the innate immune system via TLR-7 on neutrophils, macrophages and dendritic cells and indirectly induces proliferation of keratinocytes (van der Fits et al. 2009). As a readout for activation by Aldara, we monitored Myeloperoxidase (MPO) activity, which increased during Aldara treatment in both WT and KO skin (Fig. 3b). In response to Aldara, the expression of Fgfbp1 increased in WT mice (2.5-fold; Fig. 3c) as did GFP activity in heterozygous GFP-reporter mice ($Fgfbp1^{+/gfp}$; 6-fold; Fig. 3d, e). Aldara treatment also induced a striking, 4.5-fold epidermal thickening (Fig. 3f, g) and expression of the inflammatory genes Il6 and Il17a as well as the epithelial marker Krt16 (Fig. 3h, S5a). The expression of these genes was significantly elevated at baseline in the skin of KO mice, indicating a skin phenotype with activated immune response and thus increased epithelial proliferation (Fig. 2b, d, 3f, g). It has been shown that the skin barrier function is highly dependent on FGF receptor expression (Yang et al. 2010). Fgfr1,2, 3, 4 expression however, were not altered significantly in total skin (Fig. S4). These data suggest that the loss of Fgfbp1 induces a baseline increase in pro-inflammatory gene expression in KO skin comparable to the Aldara treatment effect in WT.

DMBA/TPA-induced skin papilloma formation is reduced and delayed in KO mice

Fgfbp1 expression is increased in mouse skin during carcinogen-induced papilloma formation (Kurtz et al. 2004) suggesting a potential role during carcinogenesis. Six week old GFP reporter mice ($Fgfbp1^{+/gfp}$) treated topically with DMBA/TPA (Fig. 4a) showed macroscopically visible GFP activity in papillomas (Fig. 4b), GFP protein expression in the more differentiated outer keratinocyte layers of the epidermis (Fig. 4c, magnified in Fig. S5b) and >2-fold GFP mRNA (Fig. 4d). In WT skin Fgfbp1 expression was induced similarly by 2.8-fold (Fig. 4k). Skin biopsies taken from carcinogen treated WT and KO mice showed a similar increase in hyperplastic keratinocyte layers as early as 12 days after the first treatment and maximal thickness at 57 days (Fig. 4e). However, the appearance of skin papillomas was significantly ($p<0.01$) delayed in KO mice: The first lesions in WT mice were found after 1.5 months (day 44) and only a month later (day 73) in the KO group (Fig. 4f, g). By day 100 all WT mice developed papilloma whereas one KO mouse remained papilloma-free until the end of the experiment (Fig. 4g). Also, the number of papilloma per mouse was significantly reduced in the KO mice (Fig. 4h).

In addition to the reduced papilloma formation, we observed an increase of ulceration in the neck region of KO mice (Fig. S6a). In earlier work, we had observed an impact of FGFBP proteins on vascular leakiness in embryonic tissues (Gibby et al. 2009) and it is known that altered vascular permeability can cause ulcerative inflammation (Nagy et al. 2008). Thus, we

evaluated papilloma tissues for vessel integrity. Quite strikingly, the number of extravasated erythrocytes was increased >3-fold in the KO mice indicating a contribution of Fgfbp1 to vascular integrity in adult tissues (Fig. 4 i, j).

Pathway activation after DMBA/TPA challenges

To complement the phenotypic analyses, we compared the impact of DMBA/TPA treatment on the gene expression profile in skin and found robust gene expression difference associated with epidermal development, immune response and extracellular matrix (ECM) (Fig. S7). Carcinogen treatment induced the activated keratinocyte-specific genes Krt16 and Sprr2d to comparable levels in both WT and KO skin. Due to the elevated level at baseline, the relative induction by carcinogen was much lower in KO versus WT skin. The same pattern was observed for the immune response gene S100a8. Its baseline level expression in untreated KO skin was 13-fold higher than the expression in WT skin and the induction by carcinogen treatment elevated its expression to similar levels in both KO and WT. Finally, the ECM protease Klk6 was upregulated at baseline by 4.3-fold in KO skin. DMBA/TPA treatment induced its expression in both WT and KO skin (Fig. 4k). Immunohistochemistry confirmed the upregulation of the Krt13 and Krt16 protein in the epidermis as well as the downregulation of Col1A2 in the dermis during DMBA/TPA treatment (Fig. S5c).

An analysis of Fgfr mRNA by qRT-PCR did not show any significant differences in b/c splice isoform expression of Fgfr1, 2 and 3 (Fig. S6b, c). Also, immunohistochemistry did not reveal any difference in keratinocyte proliferation between WT and KO (Fig. S5c, d). Pathway analysis of the global gene expression patterns revealed that carcinogen treatment activated Tight Junction Signaling, Agranulocyte Adhesion, Extravasation and Diapedesis, Epithelial Adherens Junction Signaling, and Role of IL-17a in Psoriasis in both WT and KO skin. These pathways are already activated at baseline in the untreated KO skin (Fig. S2a, b, c). Upstream regulators that are significantly altered with a z-score above 2 include Tnf, LPS, Ifn-γ, Nfκb, Cebp-α, Tgf-β1, all of which are involved in cancer pathways as well as inflammatory responses (Fig. S2d, e).

Fgfbp1 expression is induced and required for timely wound healing

We have previously found that conditional transgenic FGFBP1 expression accelerates wound healing (Tassi et al. 2011). Complementary to that we observed a significant three-day delay in full-thickness skin wound healing in KO mice (Fig. 5a, b). This supports a significant contribution of endogenous Fgfbp1 to timely wound healing. Fgfbp1$^{+/gfp}$-reporter mice showed maximal levels of GFP fluorescence adjacent to the wounds on day 4 (Fig. 5c, d). This was corroborated by IHC that showed a high expression of GFP protein close to the wounds and a low expression at remote skin (Fig. S8a). Fgfbp1-expressing cells were identified as hyperpoliferating keratinocytes and inflammatory cells in the granulation tissue (Fig. 5e magnified in Fig. S8b). Microscopic analysis of wounds on day four (Fig. 5f, magnified in Fig. S8c) showed that the reëpithelialization of wounds in the WT mice was more advanced (Fig. 5g). Also, the granulation tissue in wounds in KO mice contained a significantly higher number of extravasated erythrocytes and fewer microvessels and capillaries than WT mice (Fig. 5h, i magnified in Fig. S8c) indicating less mature

angiogenesis. There was a slight decrease in total cells in the granulation tissue of KO mice (Fig S8d) though no difference in their proliferation index (Fig. S8e, f).

Fgfbp1-expressing cells are recruited to healing wounds

To investigate the expression of Fgfbp1 in cells recruited to healing wounds versus tissue resident cells we transplanted skin from WT donors onto the back of Fgfbp1$^{+/gfp}$ recipient mice. The transplanted skin was wounded and the fluorescence of the wound and the surrounding transplant tissue was monitored (Fig. 6a). The inside of wounds in wild type skin transplanted to Fgfbp1$^{+/gfp}$ recipient mice started to fluoresce during wound healing even when surrounded by the non-fluorescent WT skin transplant (Fig. 6b, c) suggesting that GFP-expressing cells from the host entered the wound as early as two days after wounding. IHC analysis of the granulation tissue in the wound confirmed the influx of GFP-positive cells from the host (Fig. 6b), thus corroborating that as late as five days after injury Fgfbp1-expressing cells localize to the wound.

In complementary experiments, Fgfbp1$^{+/gfp}$ skin transplanted and wounded on a WT recipient showed increased GFP activity at edge of a wound as it healed but the GFP activity inside the open wound did not increase significantly (Fig. S9a-d). These results suggest the contribution of circulating cells from the host to the wound healing of the transplant and we thus tested that next in a separate experimental setting.

To test whether bone marrow can provide Fgfbp1-expressing (GFP positive) cells via the circulation to a healing wound, we isolated bone marrow cells from Fgfbp1$^{+/gfp}$ mice and transplanted those into WT mice with skin wounds (Fig. 6d). GFP fluorescence in the wounded area peaked at days two and three after wounding (Fig. 6e, f) and sections of the wounds showed strong GFP staining of cells in the granulation tissue (Fig. 6e, magnified in Fig. S9e). These transplant experiments demonstrate that Fgbp1-expressing cells home to the wound from both the circulation and adjacent tissue and reveal that Fgfbp1-expressing bone marrow-derived cells are recruited to healing wounds.

Endogenous Fgfbp1 contributes to neoangiogenesis

Subcutaneous matrigel plugs are a well-defined model of neoangiogenesis that mimics part of the wound healing process and is driven by the invasion of monocytic cells recruited from the circulation (Anghelina et al. 2004). In earlier studies FGFBP1 was found expressed in tissue resident monocytes / macrophage (Ray et al. 2014) and gain-of-function studies had shown that expression of FGFBP1 enhances neoangiogenesis in a matrigel plug model (Tassi et al. 2011). In Fgfbp1-KO mice, a significant 3-4-fold reduction of cells that fully invade the matrigel plug and reach the center was observed. It is noteworthy that similar numbers of infiltrating cells were observed at the edges of the plugs (regions 1 and 5; Fig. 6g, h). Examination of matrigel plugs in Fgfbp1$^{+/gfp}$ reporter mice revealed a strong GFP staining of the majority of invasive cells. A large percentage of the Fgfbp1-expressing cells were inflammatory cells with multilobular nuclei (Fig. S9f).

Additional phenotypic analysis of FGFBP1-KO mice

Fgfbp1-KO mice were viable and fertile and did not show any gross phenotypic abnormalities. The expected Mendelian ratio of the offspring indicated a lack of embryonic lethality in mice in contrast to chick embryonic development where FGFBP1 is crucial for survival (Gibby et al. 2009). To detect subtle phenotypic changes, we subjected a cohort of WT and KO animals to a systematic and comprehensive characterization for 550 parameters that include behavior, neurology, morphology, metabolism, hematology and immunology (Fuchs et al. 2009). In summary of the analyses detailed in Tables S1 to S21, and Figs. S10 to S15, we found significant phenotypic alteration in KO mice in the ratio of fat versus lean body mass, food intake, spleen and heart weights, blood glucose, cholesterol, iron binding capacity, lactate, urea, serum IgG3 and IgE, behavioral tests, and in the auditory brain stem response.

Discussion

Previous studies have shown that FGFBP1 interacts with FGF1 and 2 as well as with members of the FGF7 subfamily i.e. FGF7, 10 and 22 (Beer et al. 2005). These FGFs are expressed in the skin and signal through the IIIb isoform of FGFRs. Indeed, FGF22-knockout mice develop fewer papilloma than WT mice during skin carcinogenesis while skin development and wound healing is not affected (Jarosz et al. 2012). Mice lacking keratinocyte Fgfr1b and Fgfr2b lose epidermal barrier function and the ability to maintain skin homeostasis (Yang et al. 2010). Also, a lack of Fgfr2b in keratinocytes made skin hypersensitive to papilloma formation (Grose et al. 2007). We have previously found that DMBA/TPA upregulates FGFBP1 in human skin grafted onto mice (Kurtz et al. 2004) and the analysis of published data shown above revealed increased FGFBP1 expression in hyperproliferative skin diseases such as psoriasis, actinic keratosis and SCC.

Here we report that endogenous Fgfbp1 plays a significant role in skin repair and carcinogenesis. While Fgfbp1-KO mice did not show any gross phenotypic abnormalities, a functional screen showed a decrease of transepidermal waterloss (TEWL) in KO mice that matches with significant thickening of the epidermal layer in KO mice. Interestingly, keratinocyte-specific deletion of Fgfr1 and Fgfr2b resulted in changes of the barrier function and ulceration of mouse skin (Yang et al. 2010). Epidermal thickening was also observed in keratinocyte Fgfr2b-knockout skin (Grose et al. 2007). Taken together, the results show that FGFBP1 expression is induced upon injury and tissue regeneration, whilst loss of FGFBP1 slows the response to injury during the DMBA/TPA induced carcinogenesis, wound healing and invasion into a matrigel plug. We found that the FGFR1c isoform is upregulated and the isoform ratio is shifted towards the mesenchymal c-isoform in the KO epidermis. This indicates that the loss of FGFBP1 causes an increase in mesenchymal expression pattern in the skin. This may contribute to the increased epithelial barrier function of KO skin and matches with the mesenchymal transition of the epidermis during carcinogenesis (Tanner and Grose 2015).

We also noticed an increase of the macrophage marker F4/80 in KO epidermis, suggesting an increase in FGFR1c-expressing inflammatory cells in the epidermis. This influx could also contribute to a shift to a more mesenchymal expression pattern in KO epidermis. It is

noteworthy that global gene expression changes in the skin of KO mice mimic the altered gene expression pattern observed after carcinogen treatment of WT skin. E.g. genes involved in epidermal development such as cytokeratins (Krt13, 16, 27, Sprr2d), immune response genes (Il6, Il17a, Il23, S100a8, S100a9) and the kallikrein peptidase, Klk6, are upregulated in the skin of KO mice. Indeed, these genes are upregulated in psoriasis (Kim et al. 2016; Schonthaler et al. 2013; Vinter et al. 2014) squamous cell carcinoma (De Heller-Milev et al. 2000; Ghosh et al. 2015; Iotzova-Weiss et al. 2015; Kishibe et al. 2007; Lessard and Coulombe 2012; Prassas et al. 2015; Reichelt et al. 2004) and in chronic wounds (Singh et al. 2016). Also, expression of the S100a8/a9 heterodimer which is thought to suppress papilloma formation (McNeill and Hogg 2014) is increased in the skin of KO mice (Fig. 4k). Overall the loss of Fgfbp1 increases the pro-inflammatory gene expression in the skin.

The deletion of FGF22 led to a delay in carcinogen-induced papilloma formation (Jarosz et al. 2012) matching with our results. Wound healing was, however, not affected in FGF22-KO mice. Also, it has been shown that lack of FGFR2b in keratinocytes leads to increased and spontaneous papilloma formation suggesting that FGFR2b functions as a tumor suppressor in the skin (Grose et al. 2007). Our results are somewhat different since we observed a strong upregulation of the mesenchymal FGFR1c in the epidermis of KO mice. This might increase the mesenchymal character of the epidermis preventing hyperproliferation of the keratinocytes in the epidermal layer of the skin. Finally, vascular leakage in papilloma and wound granulation tissues in KO mice is reminiscent of vascular leakage after FGFBP1 knock-down in chicken embryos (Gibby et al. 2009).

The Fgfbp1$^{+/gfp}$ reporter mice allowed us to distinguish between the contribution of locally resident and systemically recruited Fgfbp1-expressing cells. In the skin transplant experiments Fgfbp1-expressing cells migrate into healing wounds as indicated by GFP activity in the granulation tissue. Furthermore, the bone marrow transplant from Fgfbp1$^{+/gfp}$ reporter mice shows that these infiltrating cells originate from bone marrow and enter the wounds via the circulation. The model also demonstrates that Fgfbp1 is an indicator of differentiation of infiltrating cells. Early during wound healing infiltrating cells are derived from the hematopoetic lineage in the bone marrow but switch to mesenchymal progenitor cells during tissue remodeling (Opalenik and Davidson 2005). In our study, during the inflammatory phase of wound healing (day 4) most of the inflammatory cells express Fgfbp1. Similarly, in the neoangiogenesis matrigel assay the majority of invasive, inflammatory cells express Fgfbp1. This corroborates previous results by us and others that FGFBP1 is expressed in tissue-infiltrating monocytes / macrophage (Ray et al. 2014).

In conclusion, our study identifies endogenous Fgfbp1 as a significant modulator of pathways that are involved in early carcinogenesis and inflammatory tissue regeneration and links Fgfbp1 expression to tissue-infiltrating inflammatory cells from the bone marrow.

Material and Methods

Mice

Mice were housed with food and water available ad libitum under standard laboratory conditions. For studies involving WT and KO mice, heterozygous breeder pairs were used

and WT and KO littermates were selected for subsequent studies. Animals were separated based on sex, but not genotype. All animal studies were approved by Georgetown University's institutional animal care and use committee and conducted according to the NIH Guide for the Care and Use of Laboratory Animals.

Generation of knockout mice

The Fgfbp1-knockout targeting vector, Fgfbp1-KO mice and Fgfbp1^{gfp} mice in a C57BL/6 and SV129 mixed background were generated by Ingenious Targeting Company and is described in the Supplemental Materials.

Transepidermal Water Loss (TEWL)

Mouse skin was analyzed in a non-invasive manner with a special Tewameter (AquaFlux-AF200) that was placed on the skin. During a short time of 60 to 90 seconds TEWL [g/(m^2h)] was recorded (Fluhr et al. 2006).

Illumina RNA expression assay and Ingenuity pathway analysis

PolyA-RNA was analyzed by the UCLA Neuroscience Genomics core utilizing an Illumina bead array (Mouse-ref8-v.2.0) system. RNA expression values were evaluated with the Ingenuity Pathway analysis software.

Separation of dermis from epidermis

The epidermis dissociation kit (Miltenyi-Biotec) was used for epidermis/dermis separation according to manufacturer's instructions.

Statistical Analyses

Prism5 (GraphPad) software was used to compare the means of two or more groups by Student's *t*-test or analysis of variance, respectively. Statistical significance was defined as $P < 0.05$. Figures legends: *, P<0.05; **, P<0.01; ***, P<0.001

An expanded Methods section is available in the Supplementary Materials and Methods.

Supplementary Material

Refer to Web version on PubMed Central for supplementary material.

Acknowledgments

This work has been funded by NIH grant P01 HL068686 to A. W. and by the German Federal Ministry of Education and Research to the GMC (Infrafrontier grant 01KX1012).

References cited

Aigner A, Ray PE, Czubayko F, Wellstein A. Immunolocalization of an FGF-binding protein reveals a widespread expression pattern during different stages of mouse embryo development. Histochem Cell Biol. 2002; 117(1):1–11. [PubMed: 11819092]

Anghelina M, Krishnan P, Moldovan L, Moldovan NI. Monocytes and macrophages form branched cell columns in matrigel: implications for a role in neovascularization. Stem Cells Dev. 2004; 13(6): 665–76. [PubMed: 15684834]

Beer HD, Bittner M, Niklaus G, Munding C, Max N, Goppelt A, et al. The fibroblast growth factor binding protein is a novel interaction partner of FGF-7, FGF-10 and FGF-22 and regulates FGF activity: implications for epithelial repair. Oncogene. 2005; 24(34):5269–77. [PubMed: 15806171]

Czubayko F, Liaudet-Coopman ED, Aigner A, Tuveson AT, Berchem GJ, Wellstein A. A secreted FGF-binding protein can serve as the angiogenic switch in human cancer. Nat Med. 1997; 3(10): 1137–40. [PubMed: 9334727]

Czubayko F, Smith RV, Chung HC, Wellstein A. Tumor-Growth and Angiogenesis Induced by a Secreted Binding-Protein for Fibroblast Growth-Factors. J Biol Chem. 1994; 269(45):28243–8. [PubMed: 7525570]

De Heller-Milev M, Huber M, Panizzon R, Hohl D. Expression of small proline rich proteins in neoplastic and inflammatory skin diseases. Br J Dermatol. 2000; 143(4):733–40. [PubMed: 11069449]

Fluhr JW, Feingold KR, Elias PM. Transepidermal water loss reflects permeability barrier status: validation in human and rodent in vivo and ex vivo models. Exp Dermatol. 2006; 15(7):483–92. [PubMed: 16761956]

Fuchs H, Gailus-Durner V, Adler T, Pimentel JAA, Becker L, Bolle I, et al. The German Mouse Clinic: A Platform for Systemic Phenotype Analysis of Mouse Models. Curr Pharm Biotechnol. 2009; 10(2):236–43. [PubMed: 19199957]

Ghosh, D., Ding, L., Sivaprasad, U., Geh, E., Biagini Myers, J., Bernstein, JA., et al. Multiple Transcriptome Data Analysis Reveals Biologically Relevant Atopic Dermatitis Signature Genes and Pathways. In: Simon, M., editor. PLoS ONE. Vol. 10. 2015. p. e0144316

Gibby KA, McDonnell K, Schmidt MO, Wellstein A. A distinct role for secreted fibroblast growth factor-binding proteins in development. Proc Natl Acad Sci USA. 2009; 106(21):8585–90. [PubMed: 19433791]

Grose R, Fantl V, Werner S, Chioni AM, Jarosz M, Rudling R, et al. The role of fibroblast growth factor receptor 2b in skin homeostasis and cancer development. EMBO J. 2007; 26(5):1268–78. [PubMed: 17304214]

Guban B, Vas K, Balog Z, Manczinger M, Bebes A, Groma G, et al. Abnormal regulation of fibronectin production by fibroblasts in psoriasis. Br J Dermatol. 2016; 174(3):533–41. [PubMed: 26471375]

Henke RT, Eun Kim S, Maitra A, Paik S, Wellstein A. Expression analysis of mRNA in formalin-fixed, paraffin-embedded archival tissues by mRNA in situ hybridization. Methods. 2006; 38(4):253–62. [PubMed: 16513366]

Iotzova-Weiss, G., Dziunycz, PJ., Freiberger, SN., Läuchli, S., Hafner, J., Vogl, T., et al. S100A8/A9 Stimulates Keratinocyte Proliferation in the Development of Squamous Cell Carcinoma of the Skin via the Receptor for Advanced Glycation-End Products. In: Hudson, BI., editor. PLoS ONE. Vol. 10. 2015. p. e0120971

Jarosz M, Robbez-Masson L, Chioni AM, Cross B, Rosewell I, Grose R. Fibroblast growth factor 22 is not essential for skin development and repair but plays a role in tumorigenesis. PLoS ONE. 2012; 7(6):e39436. [PubMed: 22737238]

Kim KE, Houh Y, Park HJ, Cho D. Therapeutic Effects of Erythroid Differentiation Regulator 1 on Imiquimod-Induced Psoriasis-Like Skin Inflammation. Int J Mol Sci. 2016; 17(2)

Kishibe M, Bando Y, Terayama R, Namikawa K, Takahashi H, Hashimoto Y, et al. Kallikrein 8 is involved in skin desquamation in cooperation with other kallikreins. J Biol Chem. 2007; 282(8): 5834–41. [PubMed: 17182622]

Kurtz A, Aigner A, Cabal-Manzano RH, Butler RE, Hood DR, Sessions RB, et al. Differential regulation of a fibroblast growth factor-binding protein during skin carcinogenesis and wound healing. NEO. 2004; 6(5):595–602.

Kurtz A, Wang HL, Darwiche N, Harris V, Wellstein A. Expression of a binding protein for FGF is associated with epithelial development and skin carcinogenesis. Oncogene. 1997; 14(22):2671–81. [PubMed: 9178765]

Lessard JC, Coulombe PA. Keratin 16–Null Mice Develop PalmoplantarKeratoderma, a Hallmark Feature of PachyonychiaCongenita and Related Disorders. J Investig Dermatol Elsevier Masson SAS. 2012; 132(5):1384–91.

McNeill E, Hogg N. S100A9 has a protective role in inflammation-induced skin carcinogenesis. Int J Cancer. 2014; 135(4):798–808. [PubMed: 24436096]

Nagy JA, Benjamin L, Zeng H, Dvorak AM, Dvorak HF. Vascular permeability, vascular hyperpermeability and angiogenesis. Angiogenesis. 2008; 11(2):109–19. [PubMed: 18293091]

Nair RP, Duffin KC, Helms C, Ding J, Stuart PE, Goldgar D, et al. Genome-wide scan reveals association of psoriasis with IL-23 and NF-κB pathways. Nat Genet. 2009; 41(2):199–204. [PubMed: 19169254]

Nindl I, Dang C, Forschner T, Kuban RJ, Meyer T, Sterry W, et al. Identification of differentially expressed genes in cutaneous squamous cell carcinoma by microarray expression profiling. Mol Cancer. 2006; 5:30. [PubMed: 16893473]

Opalenik SR, Davidson JM. Fibroblast differentiation of bone marrow-derived cells during wound repair. FASEB J. 2005; 19(11):1561–3. [PubMed: 16014399]

Prassas I, Eissa A, Poda G, Diamandis EP. Unleashing the therapeutic potential of human kallikrein-related serine proteases. Nature reviews Drug discovery. 2015; 14(3):183–202. [PubMed: 25698643]

Ray PE, Al-Attar A, Liu XH, Das JR, Tassi E, Wellstein A. Expression of a Secreted Fibroblast Growth Factor Binding Protein-1 (FGFBP1) in Angioproliferative Kaposi Sarcoma. J AIDS Clin Res. 2014; 05(06)

Reichelt J, Furstenberger G, Magin TM. Loss of keratin 10 leads to mitogen-activated protein kinase (MAPK) activation, increased keratinocyte turnover, and decreased tumor formation in mice. J Invest Dermatol. 2004; 123(5):973–81. [PubMed: 15482487]

Reischl J, Schwenke S, Beekman JM, Mrowietz U, Stürzebecher S, Heubach JF. Increased expression of Wnt5a in psoriatic plaques. J Invest Dermatol. 2007; 127(1):163–9. [PubMed: 16858420]

Schonthaler, HB., Guinea-Viniegra, J., Wculek, SK., Ruppen, I., Ximénez-Embún, P., Guío-Carrión, A., et al. Immunity. Vol. 39. Elsevier Inc; 2013. S100A8-S100A9 Protein Complex Mediates Psoriasis by Regulating the Expression of Complement Factor C3; p. 1171-81.

Singh K, Agrawal NK, Gupta SK, Sinha P, Singh K. Increased expression of TLR9 associated with pro-inflammatory S100A8 and IL-8 in diabetic wounds could lead to unresolved inflammation in type 2 diabetes mellitus (T2DM) cases with impaired wound healing. J Diabetes Complicat. 2016; 30(1):99–108. [PubMed: 26525587]

Stern RS. Psoriasis. The Lancet. 1997; 350(9074):349–53.

Tanner Y, Grose RP. Dysregulated FGF signalling in neoplastic disorders. Seminars in Cell and Developmental Biology. 2015

Tassi E, Wellstein A. The angiogenic switch molecule, secreted FGF-binding protein, an indicator of early stages of pancreatic and colorectal adenocarcinoma. Semin Oncol. 2006; 33(6):S50–6. [PubMed: 17178288]

Tassi E, McDonnell K, Gibby KA, Tilan JU, Kim SE, Kodack DP, et al. Impact of fibroblast growth factor-binding protein-1 expression on angiogenesis and wound healing. Am J Pathol. 2011; 179(5):2220–32. [PubMed: 21945411]

van der Fits L, Mourits S, Voerman JSA, Kant M, Boon L, Laman JD, et al. Imiquimod-Induced Psoriasis-Like Skin Inflammation in Mice Is Mediated via the IL-23/IL-17 Axis. J Immunol. 2009; 182(9):5836–45. [PubMed: 19380832]

Vinter H, Iversen L, Steiniche T, Kragballe K, Johansen C. Aldara-induced skin inflammation - studies of psoriasis patients. Br J Dermatol. 2014

Walter A, Schaefer M, Cecconi V, Matter C, Urosevic-Maiwald M, Belloni B, et al. Aldara activates TLR7-independent immune defence. Nature Communications. 2013; 4

Yang J, Meyer M, Müller AK, Böhm F, Grose R, Dauwalder T, et al. Fibroblast growth factor receptors 1 and 2 in keratinocytes control the epidermal barrier and cutaneous homeostasis. J Cell Biol. 2010; 188(6):935–52. [PubMed: 20308431]

Abbreviations

DMBA	7,12-dimethylbenz[a]anthracene
FGFBP	Fibroblast Growth Factor Binding Protein
KO	knockout
qRT-PCR	quantitative real-time PCR
TEWL	Transepidermal water loss
TPA	12-O-tetradecanoyl-phorbol-13- acetate
WT	wildtype

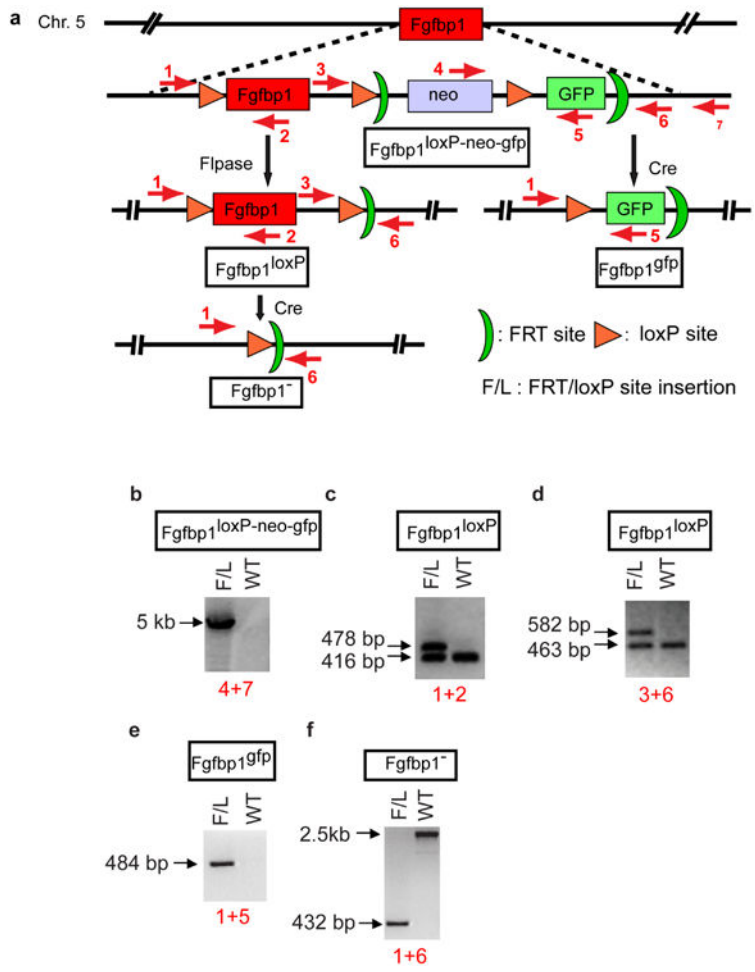

Figure 1. Generation of Fgfbp1 KO and GFP-knock-in mice

(**a**) Schematic of the knockout strategy for the Fgfbp1 gene depicts the endogenous locus of the Fgfbp1 gene on chromosome 5 and the targeting construct below. Mice with the targeted insertion of a floxed Fgfbp1 Neo and Gfp cassette in the Fgfbp1 locus ($Fgfbp1^{loxP\text{-}neo\text{-}gfp}$) were crossed with Cre expressing mice resulting in an insertion of a GFP reporter allele ($Fgfbp1^{gfp}$), or with FLPase mice resulting in a floxed Fgfbp1 ($Fgfbp1^{loxp}$) allele. $Fgfbp1^{loxP}$ mice were further crossed with cre-mice to generate Fgfbp1-KO mice ($Fgfbp^{-/-}$, KO). Numbered arrows depict locations of genotyping primer (Suppl. Table S22). (**b-f**) PCR analysis of genomic DNA isolated from tail snips. (**b**) Primers 4 and 7 resulted in an amplicon of 5000 bp only in the allele with the floxed Fgfbp1 Neo and GFP cassette. (**c**) Primers 1 and 2 resulted in an amplicon of 478 bp with the 5′loxP site in the floxed Fgfbp1 allele and 416 bp in the WT allele. (**d**) Primers 3 and 6 resulted in an amplicon of 582 bp with the 3′loxP site in the floxed Fgfbp1 allele and 463 bp in the WT allele. (**e**) Primers 1 and 5 resulted in an amplicon of 484 bp only in the GFP reporter allele. (**f**) Primers 1 and 6 resulted in an amplicon of 432 bp in the KO allele and 2.5kb in the WT allele.

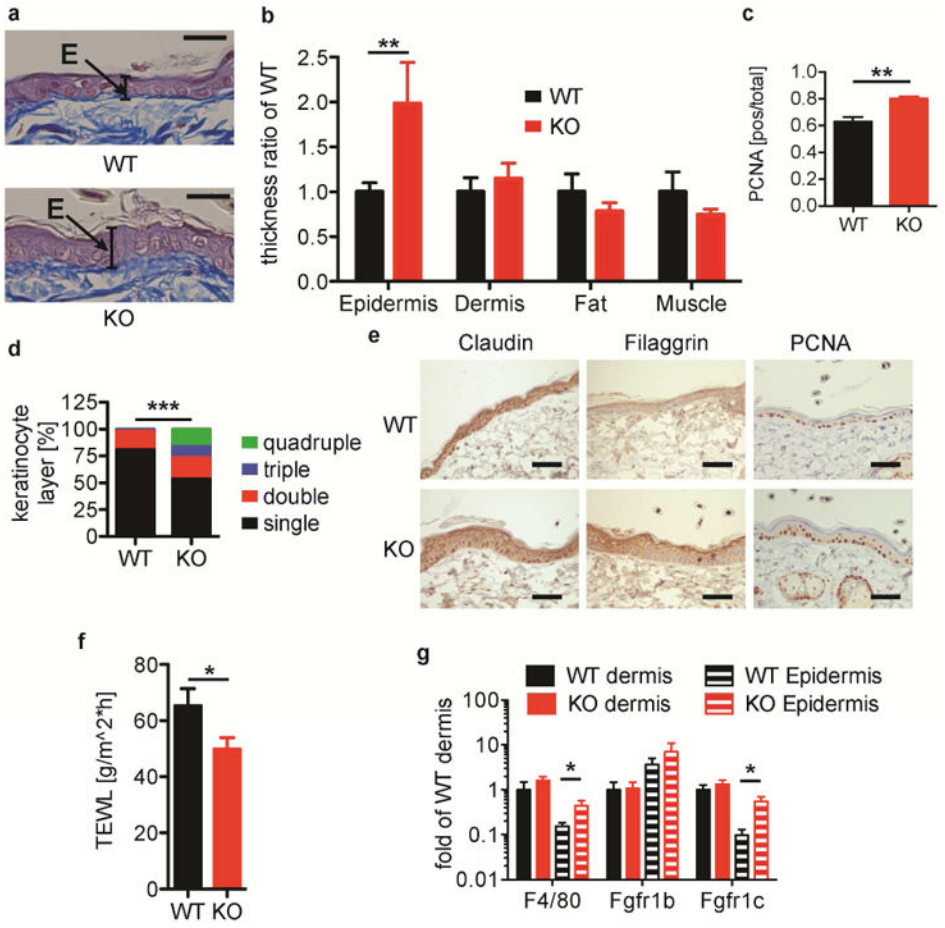

Figure 2. Fgfbp1-KO mouse epidermis is thicker and has reduced permeability

(**a,b**) Representative high magnification pictures of Masson's trichrome stained tissue section of skin from WT and KO mice shows a thicker epidermal layer (E) in KO mice. (**b**) In contrast to the epidermis, dermis, fat layer and muscle are not significantly different. (Mann Whitney test, WT n=5; KO n=6; 20 fields per skin sample). (**c**) Proliferation of basal keratinocytes in KO epidermis is higher than in WT (PCNA positive nuclei, Student's t test, n=5). (**d**) Nucleated keratinocyte layers in KO epidermis contain multiple strata whereas WT epidermis is mostly a monolayer (Chi-square test, n=3), (**e**) Representative images of skin section stained for Claudin 1, Filaggrin, PCNA (scale bar = 100 μm). (**f**) Transepidermal water loss (TEWL) was decreased in male KO compared to WT males (Student's t test, WT n=14; KO n=15). (g) RNA expression in separated dermis and epidermis (Student's t test, WT n=4; KO n=3).

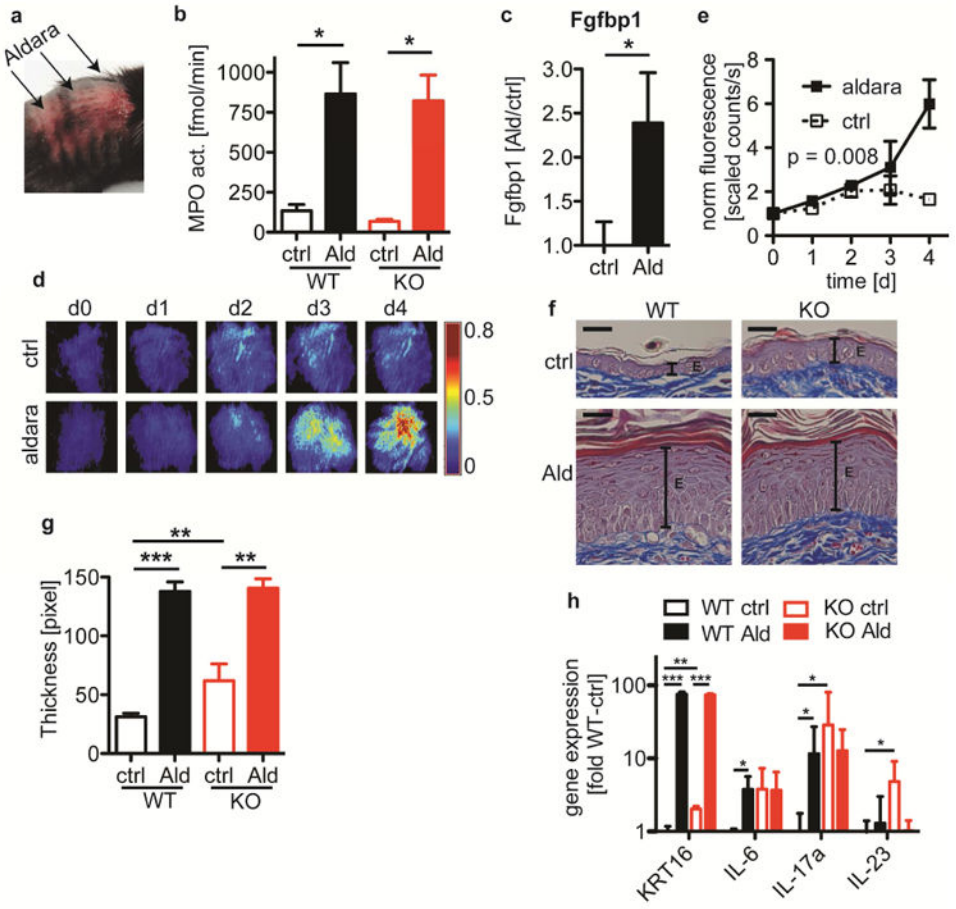

Figure 3. Effect of topical Aldara treatment

(**a**) Daily treatment of shaved back skin of Fgfbpl^{ggp} mice for 4 days. Skin turned red as the inflammation progresses. (**b**) Myeloperoxidase (MPO) activity (Student's t-test, WT n=4; KO n=5). (**c**) Induction of Fgfbpl expression in WT skin. (**d**) GFP fluorescence in Aldara and ctrl (vaseline) treated mice for 5 days. Fluorescence intensity is shown as scaled counts/s in a heatmap from 0 (black) to 0.8 (dark red). (**e**) Quantification of GFP-fluorescence in panel **b** (Chi-square, n=2). (**f**) Masson's trichrome stained tissue sections of WT and KO epidermis (scale bar = 50 μm). (**g**) Quantification of the thickness of the epidermis (Student's t-test, n=7). (**h**) Effect on mRNA expression of Krtl6,116,1117a and 1123. (Student's t test, n=7)

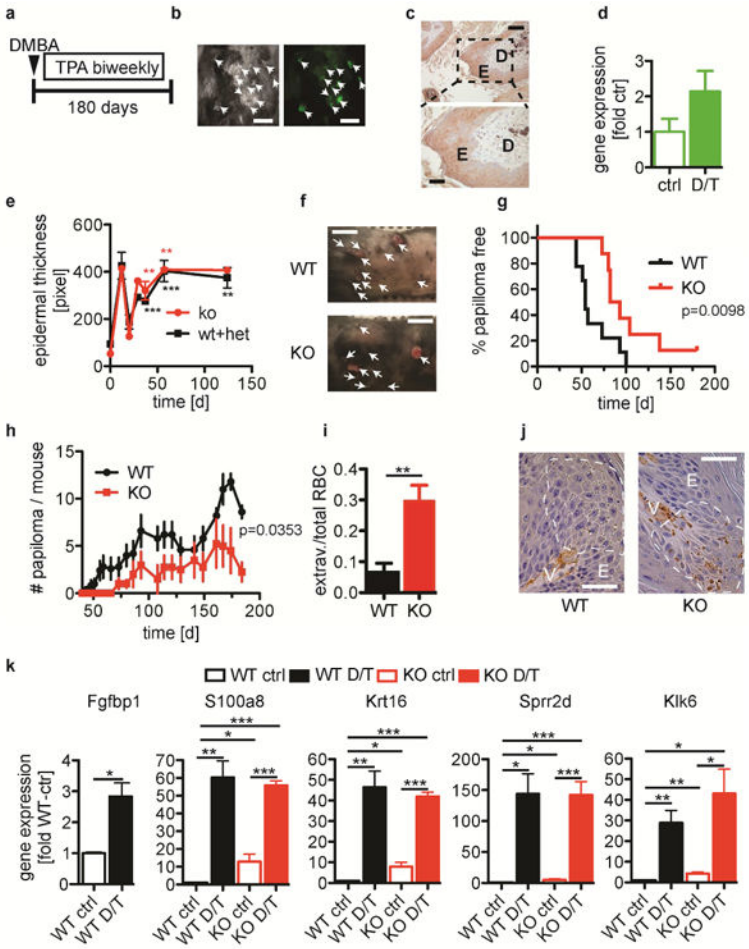

Figure 4. DMBA/TPA (D/T) effects are delayed in Fgfbp1-KO mice

(**a**) Treatment scheme: A single topical treatment with DMBA was followed by biweekly TPA treatments for 180 days. (**b**) In vivo fluorescence of Fgfbpl $^{+/gfp}$ mouse skin after 180 days of treatment shows GFP activity in papillomas. Visible (left panel) and green fluorescence channels (right panel) are shown. Arrows indicate papillomas (scale bar = 5 mm). (**c**) Immunostaining of representative tissue sections with anti-GFP antibody shows staining of the epidermis (E) excluding the basal layer of keratinocytes. (Dermis (D), scale bar =200 μm (top panel), 100 μm (bottom panel), magnified in Suppl. Fig. S5b). (**d**) GFP RNA expression in Fgfbpl$^{+/gfp}$ mice after 180 days of treatment (n=3). (**e**) The thickness of the epidermal layer progressively increased upon treatment. Biopsies were taken and the epidermal thickness was measured. On days 57 and 124 only papilloma-free skin sections were measured. (**f**) Papilloma on day 161. (**g**) Kaplan-Meier plot of papilloma occurrence ($p<0.01$; Mantel-Cox test, WT n=9; KO n=8). (**h**) Papilloma frequency (2-way ANOVA, WT n=9; KO n=8). (**i**) Vascular leakiness in papilloma indicated by extravasated erythrocytes (student's t-test, n=5, 35 fields per sample). (**j**) Representative anti CD31-stained tissue section; E=epidermis, V=vessel; interrupted white line surrounds area with extravasated erythrocytes (scale bar = 100 μm). (**k**) Illumina bead array analysis of DMBA/TPA treated skin shows induction of Fgfbp1 (left panel) and increased expression of S100a8, Krt16,

Sprr2d and Klk6. Baseline expression is higher in Fgfbp1-KO skin but induced upon DMBA/TPA treatment (Student's t-test, WT n=4; KO n=3).

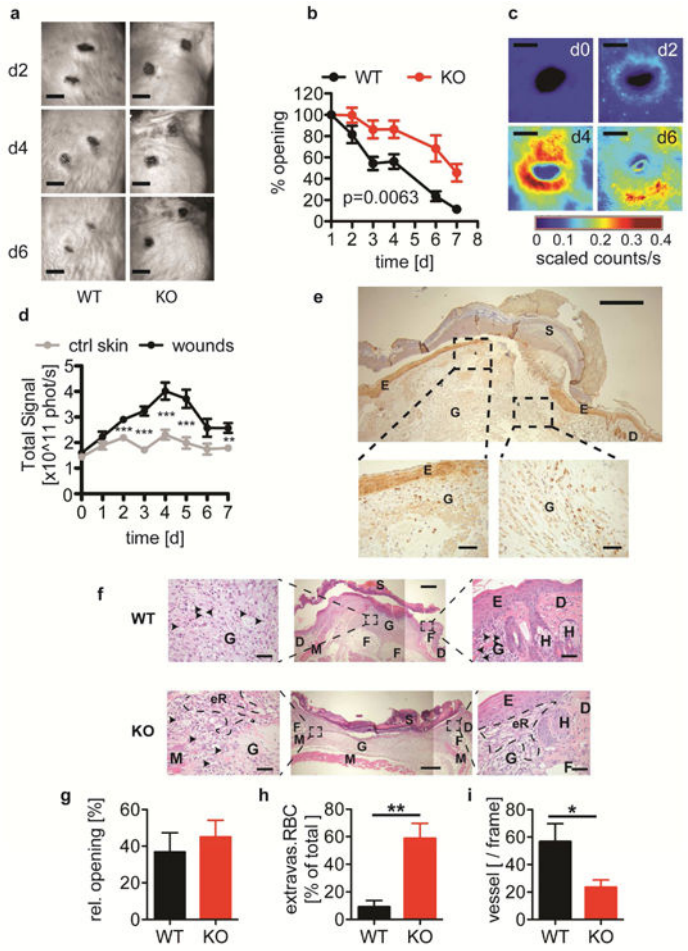

Figure 5. Wound healing is delayed in Fgfbp1-KO mice

(**a**) The back skin of WT and KO mice was wounded on day 0 and wound sizes were measured daily for 7 days (scale bar = 5 mm). (**b**) Quantification of wound sizes (2-way Anova, WT n=20; KO n=12). (**c**) Activation of the Fgfbp1 expression during wound healing indicated by fluorescence in Fgfbp1$^{+/gfp}$ mouse skin. Heat map images are shown (scale bar = 2.5 mm). (**d**) GFP quantitation after wounding. GFP fluorescence peaks on day 4 (student's t-test for each time point, n=10). (**e**) Immunostaining of representative tissue sections with anti-GFP antibody (scale bar = 1 mm, magnified scale bar 100 μm, higher magnification in Suppl. Fig. S8b). (**f**) Representative images of hematoxylin/eosin stained wounds (scale bar = 1 mm), magnified sections show extravasated red blood cells (eR), single erythrocytes (arrow heads); (scale bar = 100 μm, granulation tissue (G), fat (F), scab (S), dermis (D), muscle (M), hair follicles/glands (H), epidermis (E) (higher magnification in Suppl. Fig S8c). (**g**) Relative opening of wounds, calculated by the ratio between wound opening divided by wound diameter (distance between collagen-containing dermis times 100, n=5). (**h**) Quantification of extravasated erythrocytes (Student's t test; WT n=5; KO n=6 wounds; means of at least 10 fields per wound). (**i**) Quantification of microvessels and capillaries (Student's t test, WT n=5; KO n=6 wounds; at least 10 fields per wound).

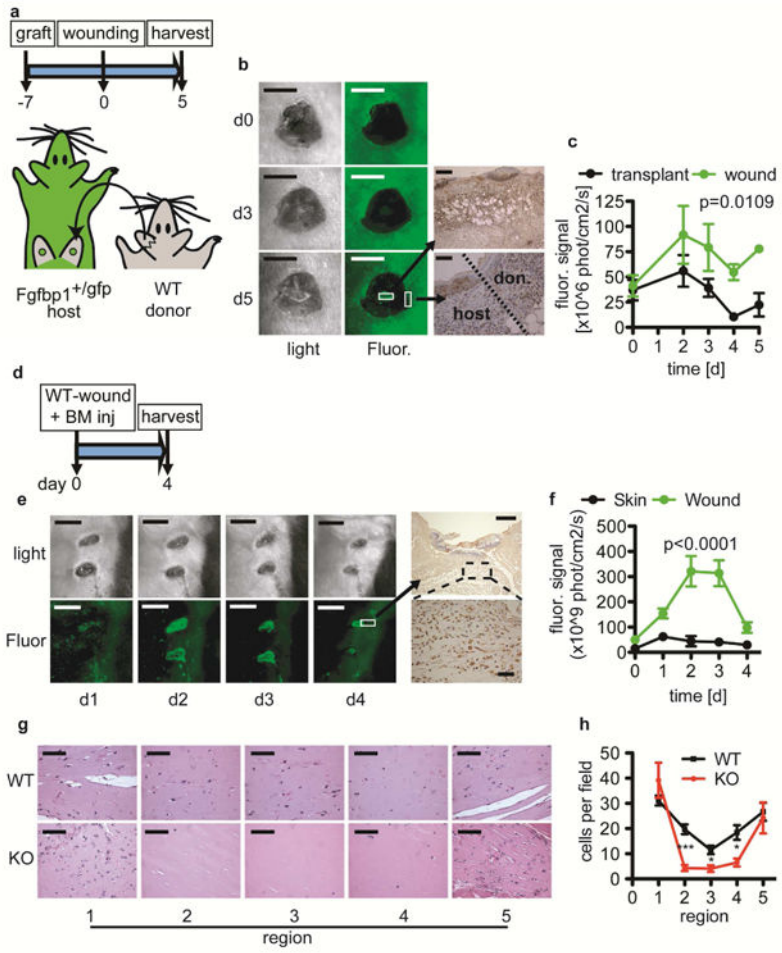

Figure 6. Fgfbp1-expressing cells migrate into wounds

(**a to c**) Host Fgfbp1 expressing cells enter wound in transplanted skin. (**a**) Time line (in days) and schematic of experiments. Skin from a WT mouse was transplanted onto the back of a Fgfbp1$^{+/gfp}$ mouse, wounded after 7 days and fluorescence monitored. (**b**) Left panels: Bright field images and GFP fluorescence during wound healing (scale bar = 5 mm). Right panels: Immunostaining of a representative tissue section with an anti-GFP antibody shows staining of inflammatory cells that entered transplanted skin wound (scale bar = 250 μm). (**c**) Quantification of GFP signal in intact and wounded skin transplant (2-way Anova, n=7). (**d to f**) Wound healing with concurrent bone marrow transplant from the Fgfbp1$^{+/gfp}$ reporter model. (**d**) Schematic of the experiment. (**e**) Bright field and GFP fluorescence images of wounds over 4 days (scale bar = 5 mm). Immunostaining of representative tissue sections with anti-GFP antibody confirmed GFP-positive cells in granulation tissue of the wound (Scale bars = 500 μm top right panel, 100 μm bottom right panel; higher magnification in Suppl. Fig. S9e). (**f**) Quantification of GFP activity; 2-way Anova, n=8. (**g**) Matrigel plug neoangiogenesis assay. H&E stained tissue sections of subcutaneously injected matrigel after 7 days in WT and KO mice. Scale bar, 100 μm. (**h**) Quantification of invasive cells per field in different regions of the matrigel. Regions 1 and 5 represent the edges of the plugs, regions 2-4 the center; WT n=12; KO n=20.